RESGOOGLEDENSE SOFT: AN EFFECTIVE ENSEMBLE MODEL

Manasa S [1] Bhavya D.N [2] Mahesha D.M [3] Sharath Kumar Y.H [4]
[1,2,3] *Department of Studies and Research in Computer Science, Karnataka State Open University, Mysore-570006, India.* [4] *Maharaja Institute of Technology Mysore, Department of ISE, MIT Mysore, India.*

***Abstract*- This work explores the analysis of chest X-ray images and proposes a machine learning ensemble model tailored for early detection of COVID-19 and pneumonia lung infections. The suggested model, RGDSoft, integrates a soft voting ensemble technique, leveraging the capabilities of pre-trained classifiers ResNet-18, GoogLeNet, and DenseNet-121 for efficient image classification. Performance evaluation of the model is conducted using two datasets: the COVID-19 dataset, consisting of 1143 positive COVID-19, 1341 normal, and 1345 pneumonia images, and the Kermany dataset, containing 5856 chest X-ray images categorized as "Pneumonia" and "Normal." The training and testing processes utilize 80% and 20% of the image set, respectively. The proposed model's efficacy is demonstrated and compared against established pre-trained models such as GoogleNet, ResNet 18, and DenseNet 121. The results showcase the superiority of the recommended ensemble model, achieving a remarkable 98.1% accuracy, 98.8% precision, and 98.8% recall on the Kermany dataset, and 94% accuracy, 96% precision, and 96% recall on the COVID-19 dataset. The novelty lies in the RGDSoft model's outperformance of various classifiers, including GoogleNet, ResNet18, and DenseNet121, across multiple metrics like accuracy, precision, and recall. Its versatility is demonstrated by its effectiveness on diverse datasets, establishing it as a robust and broad-ranging model in the field.**

1. INTRODUCTION

Acute Respiratory Syndrome with Severity the sickness known as Covid19 is brought on by the coronavirus 2 (SARS CoV-2). Zoonotic bacteria are contagious infections that cause significant deterioration of the respiratory organs, which they first spread to animals before reaching humans. 2019 saw the discovery of the first COVID case in the Chinese city of Wuhan. The World Health Organization proclaimed a global epidemic due to this lethal virus (WHO). The most typical signs of COVID19 are fever, a dry cough, and tiredness. As of February 28, 2022, COVID-19 has reached every corner of the globe, claiming the lives of 6,004,421 individuals and impacting 446,511,318 people worldwide. Reverse transcription- polymerase chain reaction (RT-PCR), a time-consuming method with a high probability of false-positive results is used to diagnose COVID-19 in humans. Currently, the excellent method for coping with the medical diagnosis systems is to learn important clinical imaging procedures. Computer-aided diagnosis methods like computed tomography and chest X-rays can be employed in addition to RT-PCR. Lung infections are routinely identified using CT and chest X-ray imaging. Although CT scans are routinely used, the expense and radiation exposure provide serious challenges for the diagnosis of COVID-19. CXR pictures should be utilized instead of CT images because they are more readily available and expose users to less radiation. See Figure 1

Consequently, in the present study, we employed deep learning algorithms to identify individuals infected with COVID-19 using chest X-ray images. A total of 15,153 photos make up our collection, including 3616 COVID-19 images, 1345 viral Pneumonia images, and 10,192 normal images.

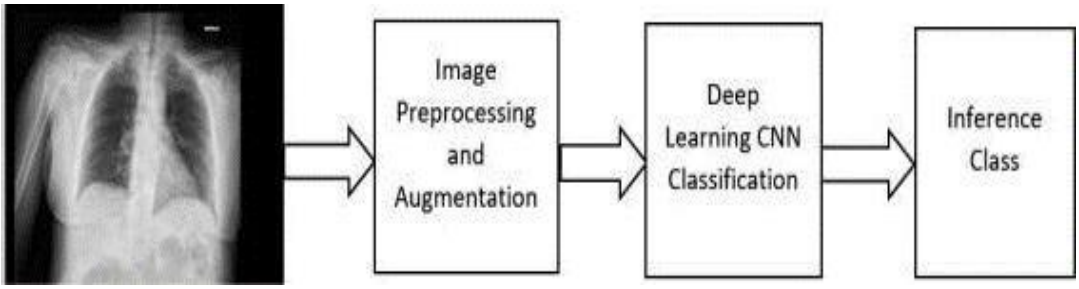

Figure 1: Screening Structure of COVID-19 and Pneumonia [9]

Although mild to moderate symptoms predominate in people with COVID-19 infections, some sometimes

experience more severe symptoms, such as pneumonia, which is distinguishable by its peripheral distribution, ground-glass opacity, fine reticular opacity, and vascular spacing. Cases of acute respiratory syndrome can result in mortality and multiple organ failure. Early detection is essential to stop the spread of SARS-COV-2, hence precise testing is required. Real-time reverse transcription polymerase chain reaction (RT-PCR) testing, which is the industry standard, costs between US$120 and US$130.

The Polymerase Chain Reaction (PCR) machine needs to be housed in a dedicated biosafety laboratory, which costs between US$ 15,000 and US$ 90,000. It is possible to employ a variety of bodily fluids, including blood, sputum, faeces, and urine. However, pharyngeal swabs, which have a positive probability of only 63%, are frequently used as samples. Because the RT-PCR has a low accuracy rate and is therefore expensive, time-consuming, and complicated to use, it is challenging to diagnose and treat patients. X-rays of the chest can be utilized to look for COVID-19 patients. They have previously been utilized to more swiftly, reliably, and economically identify pneumonia as well as the MERS and SARS-COV-1 coronaviruses. COVID-19 results in radiographic evidence of lung lesions in the lower respiratory tract even in people who do not have clinical pneumonia, which favours the detection of a broader group of contaminated individuals by radiography. Because the damaged parts of the lung may resemble those of other types of pneumonia, it is crucial to distinguish between the COVID-19 pneumonia radiographs and those of individuals with other types of pneumonia.

Computer-Aided Diagnosis (CAD) systems can decrease observational errors and, as a result, false-negative rates, facilitating quick screening for SARS-COV-2- caused pneumonia and reducing the burden of medical professionals. In this case, COVID-19 pneumonia has been identified in X-ray pictures using Deep Learning algorithms. These studies produce noteworthy outcomes, achieving more than 90% accuracy in the COVID-19 pneumonia classification.

2. RELATED WORK

Schroeder JD et al. [1] reveals that a CNN Image Model, trained with physiological data (PFTs), exhibits enhanced COPD prediction compared to an NLP Model assessing radiologist text reports trained with PFTs. This innovative approach to comparing models is a unique method for evaluating obstructive lung disease identification on chest radiographs. The study's findings, employing deep learning to predict airflow obstruction on routine chest radiographs, align with the objective of enhancing disease detection. The results indicate that a CNN model trained on physiological lung function data can complement clinical radiologist reports, leading to improved COPD identification. This is particularly significant given the underdiagnosis of COPD, which is also a risk factor for lung cancer. Xiong et al. [2] created a Deep Neural Network (DNN) for the identification of acid-fast-stained Mycobacterium tuberculosis bacilli in digital cytology slides. The challenges encountered were related to the small size of the bacilli (20×4 pixels) and the loss of resolution during digital image scanning. Despite achieving a commendable sensitivity of 98% through algorithm adjustments, the presence of contaminant bacilli and slide artifacts led to some false positive outcomes, yielding a specificity of 84%. González et al. [3] utilized a Deep Neural Network (DNN) trained on four-slice CT montages from 7983 participants in the COPD Gene study. The algorithm exhibited an accurate diagnosis of COPD with an AUC of 0.856. Subsequent research using the same dataset indicated that a DNN's staging of emphysema, ranging from 'absent' to 'advanced destructive,' strongly predicted both survival and lung function. Additionally, DNNs have been designed for the diagnosis and assessment of thrombus burden in acute pulmonary embolism. Liu et al.'s [4] algorithm achieved an AUC of 0.926 for pulmonary embolism diagnosis, and the clot burden determined by the DNN showed significant correlations with manually assessed scores (Qanadli and Mastora) and measures of correct ventricular function. Moreover, interstitial lung disease has been diagnosed through the use of machine learning algorithms. A Deep Neural Network (DNN) was used by Walsh et al. [5]; it was trained on 420,096 montages, each of which was made up of four transverse CT scans. The entire high-resolution

CT scans of 210 individuals with typical interstitial pneumonia (UIP), 392 with potential UIP, and 327 with scans thought to be inconsistent with UIP were used to create these montages. An experienced thoracic radiologist with expertise in interstitial lung disease set the reference standard for every CT scan. The programme showed 76.4% accuracy in a test set including 68,093 montages from 139 distinct patients. Another test set comprised 150 four-slice montages from CT scans that had previously been evaluated by 91 thoracic radiologists, with the radiologists' consensus serving as the reference standard. The algorithm's accuracy in this set was 73.3%, which is similar to the median accuracy of radiologists working individually (70.7%). Furthermore, in a Cox regression study, the equivalent Hazard Ratio (HR) for death for a majority radiologist opinion identifying UIP was 2.74. In contrast, a DNN diagnosis of UIP was linked to an HR for mortality of 2.88 when compared to a diagnosis of "not UIP." Demir F. et al. [6] address the critical public health concern of the automatic diagnosis of lung diseases. Although a large body of research has been done on this subject, there aren't many difficult datasets for lung sound categorization that include noises, background sounds, and different sampling frequencies. Furthermore, a large fraction of the current research uses conventional techniques. In order to improve classification performance in lung sound recognition, deep learning-which is regarded as a cutting-edge technique is used in this study. Using a colormap to extract deep features, the suggested method's preprocessing step creates images with one-to-one spectrogram qualities, which are then fine-tuned. Both deep learning methodologies employed the VGG-16 architecture of Convolutional Neural Network (CNN) for extracting features. Furthermore, the classification performance was assessed using the AlexNet and ResNet-50 models of CNN, and the VGG-16 model was chosen for the proposed techniques due to its higher classification accuracy. The classification accuracies of both proposed methods showed substantial improvement when applied to the ICBHI 2017 Database, known for its challenging-to-classify lung sounds. In comparison to other published methods, the first proposed method, employing deep feature extraction and an SVM classifier, demonstrated a noteworthy increase in classification accuracy by 7.62%. Similarly, the second proposed method, incorporating transfer learning and a softmaxclassifier, achieved a 5.18% improvement in classification accuracy. Gite S. et al. [7] trained four segmentation models using the Shenzhen and Montgomery datasets and assessed their performance based on various metrics, including accuracy, precision, sensitivity, specificity, recall, mean_iou, and dice_coefficient. Given the crucial role of segmented images in accurate disease diagnosis, the authors present the results of image segmentation. The U-Net++ algorithm emerged as the top performer in this study, producing segmented images with a dice_coefficient of 0.9796, mean_iou of 0.9598, and accuracy of 0.9874. While U-Net also demonstrated acceptable results, segmenting lungs with a dice_coefficient of 0.9217, mean_iou of 0.8572, and accuracy of 0.9555, SegNet's performance was deemed unsatisfactory. Even though all the models in this research exhibit an architecture comprising an encoder followed by a decoder, the superior performance of U-Net++ can be credited to its redesigned skip pathways, dense skip connections, and deep supervision. As a result, U-Net++ emerges as the most efficient model for segmenting chest X-ray images Zak M et al. [8] developed a pipeline for classifying lung diseases using transfer learning, which they applied to small datasets of lung images. They assessed its efficacy in classifying both non-segmented and segmented chest X-ray images. In their most effective framework, they incorporated the U-net segmentation network and the InceptionV3 deep model classifier. Their frameworks were contrasted with existing models, showing that models pre-trained through transfer learning and straightforward classifiers like shallow neural networks can effectively rival complex systems. According to existing literature, a variety of lung disease prediction systems have been developed using machine learning and deep learning approaches, each offering varying levels of accuracy. The performance of these systems is influenced by factors such as feature selection techniques, machine learning and deep learning algorithms, and preprocessing methods. Developing a highly effective early diagnosis system for detecting lung diseases requires careful consideration of appropriate deep learning models, preprocessing techniques, features, and

classifiers

3. METHODOLOGY

The model architecture has a multi-level structure. Fundamentally, we made use of two freely accessible databases. The resulting chest X-ray images are next put through a second degree of processing. The third level of functionality of the recommended ensemble machine learning model is in the duty of choosing the features from previously processed chest X-ray pictures, and the fourth level of functionality is in charge of developing and putting into practice the ensemble machine learning paradigm.
Using innovative techniques, the model's usefulness and effectiveness in detecting pneumonia and coronavirus disease-19 were experimentally assessed (Figure 2).

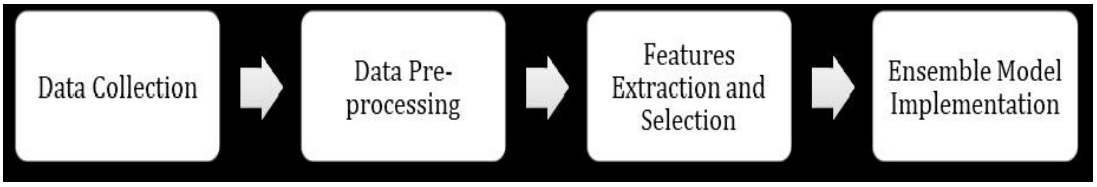

Figure 2: Methodology of the Ensemble Technique

3.1 Dataset

The findings of the analysis of the suggested system are presented in this section. Two publicly available chest X-ray datasets were used to create the COVID-19 and pneumonia datasets. The Kermany dataset [110] contains 5856 chest X-ray images evenly divided into two groups: "Pneumonia" and "Normal," taken from a sizable population of both adults and children. In comparison, the COVID-19 dataset includes 1341 normal photos, 1345 images of pneumonia, and 1143 images that are COVID-19 positive.
The suggested system was contrasted with current models and widely applied ensemble methods described in the literature to demonstrate its advantages. Additionally, we tested our method on a dataset of 5863 pictures from Germany that were split into two categories: normal and pneumonia.

4. PROPOSED METHOD

We created an ensemble framework (Figure 3) with three classifiers: GoogLeNet[111], ResNet-18[112], and DenseNet-121 using a soft voting ensemble technique. This section presents the suggested "RGDSoft" model.

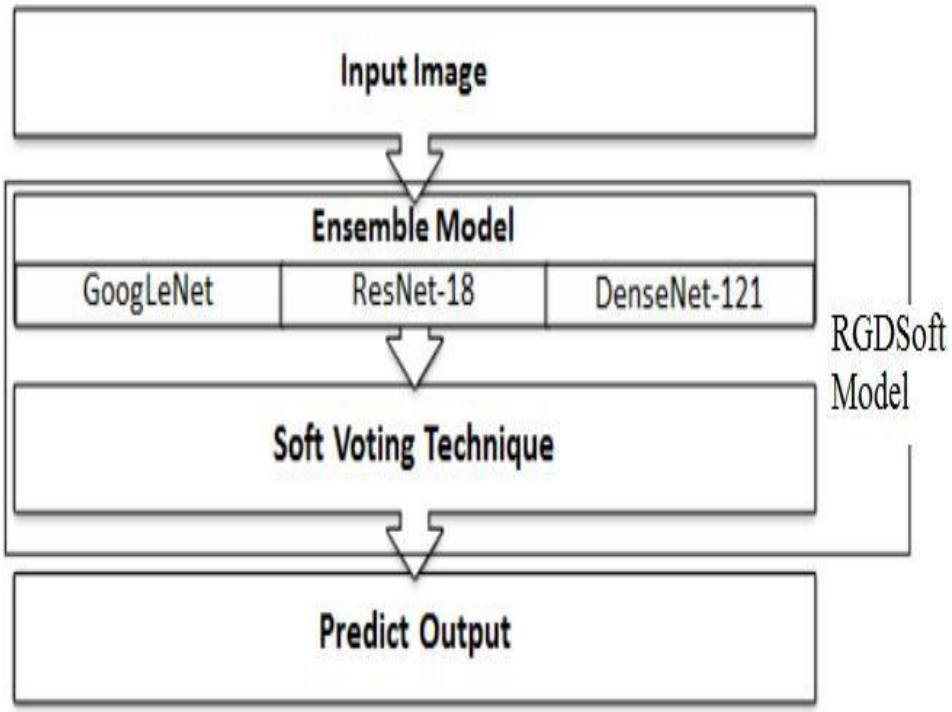

Figure 3: Proposed RGDSoft Model

4.1 GoogLeNet

In contrast to the GoogLeNet design's evenly expanding layers, Szegedy et al. [137] deep neural network is composed of "inception modules". To cope with the growing number of parameters, an inception block accommodates multiple units at each level through the simultaneous inclusion of convolution and pooling layers. The GoogLeNet model addresses computational complexity by incorporating dimension reduction inception blocks, deviating from the less efficient inception blocks found in other models [114]. The success of GoogleNet, leveraging the inception block, demonstrates how an efficient yet sparse architecture constructed from easily accessible dense building blocks improves the performance of artificial neural networks in computer vision tasks. This is a description of GoogleNet's primary components and architecture (See Figure 4)

- *Inception Modules:*

The main principle of the Inception design is to concatenate the outputs of different filter sizes simultaneously (1x1, 3x3, and 5x5) within a single layer. As a result, the network is able to simultaneously record features at many scales and levels of abstraction. Each Inception module is made up of several branches that use various filter sizes, each of which is followed by the concatenation of its outputs.

- *1x1 Convolutions:*

1x1 convolutions, commonly referred to as bottleneck layers or network-in-network layers, are widely used in Google Neural Network. By utilizing fewer input channels before applying larger convolutions, these convolutions assist in lowering the computational cost. They serve as feature fusion sites as well, allowing the network to effectively capture cross-channel correlations.

- *Max-Pooling and Dimensionality Reduction*

Downsampling the spatial dimensions of the feature maps and capturing dominating features are done using max-pooling layers. To capture features at various scales, several Inception modules support 3x3 and 5x5 max-pooling operations. After max- pooling, dimensionality reduction with 1x1 convolutions is frequently used to lower the number of channels and manage computational complexity.

- *Auxiliary Classifiers*

GoogLeNet uses auxiliary classifiers at intermediary layers to reduce the vanishing gradient issue and regularise the training process. These auxiliary classifiers consist of 1x1 convolutions followed by fully connected layers, global average pooling, and softmax outputs. During training, they contribute to the ultimate loss function and motivate the intermediate layers to pick up more significant characteristics.

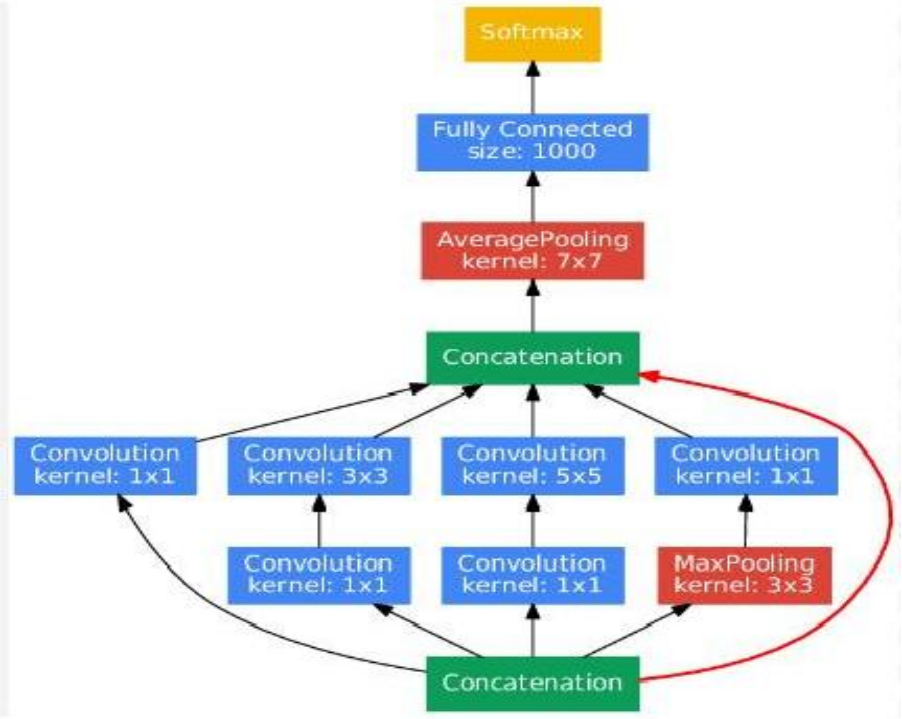

Figure 4:Basic diagram of GoogLeNet [115]

4.2 ResNet-18

He et al. [116] introduced the groundbreaking ResNet-18 model at the National University of Standards and Training for Artificial Intelligence, marking it as the inaugural creation of its kind. ResNet-18 embraces a residual learning framework, elevating the effectiveness of deep network training.
Unlike the inherent unreferenced mapping in continuous progressive convolutions, ResNet models utilize residual blocks, facilitating network augmentation and thereby enhancing model accuracy. These residuals, also known as "skip connections," enable identity mapping without requiring extra parameters or added processing complexity, as depicted in Figure 5.

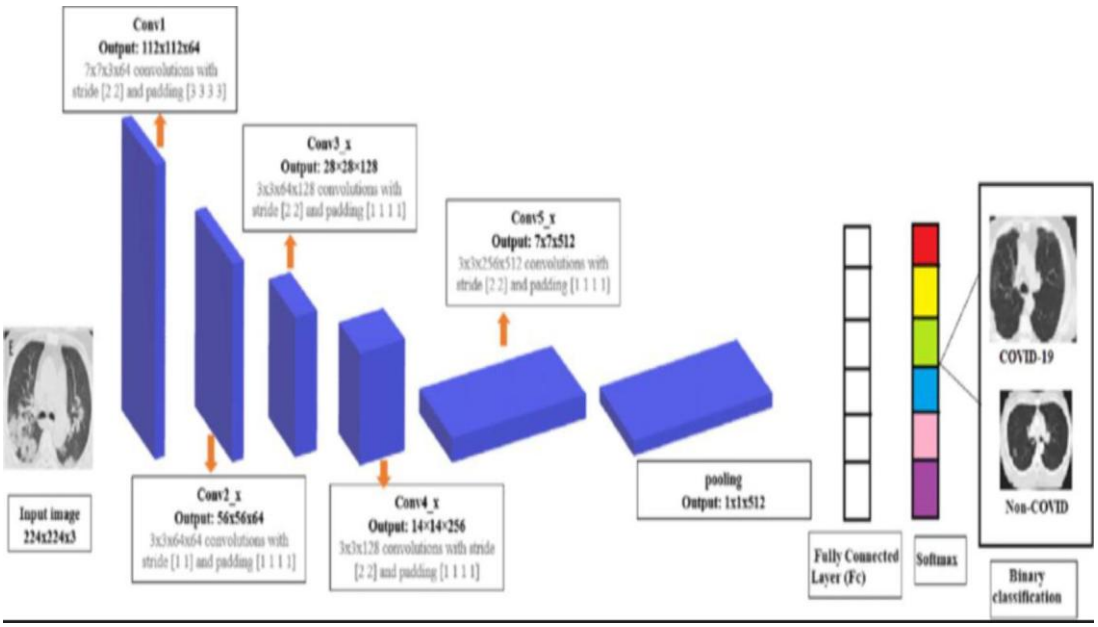

Figure 5: ResNet18 Architecture Block Diagram[117]

4.3 DenseNet-121

Machine learning tasks, including image analysis, frequently use the DenseNet-121 deep convolutional neural network design. It was introduced to deal with issues with deep neural network vanishing gradients, information flow, and effective parameter utilization. The purpose of DenseNet-121 is to perform tasks involving the classification of incoming photos into predetermined categories. The model [118] is more computationally effective and has less trainable parameters. Each DenseNet model layer's feature mappings are coupled with those of the layers before it. Feature representation is improved by joining feature maps from earlier layers with the current layer. DenseNet-121 is composed of a number of dense blocks, transition layers, a global average pooling layer, and a softmax layer for classification. See Figure 6.

- *Dense Block*

The dense block is the main component of DenseNet. It consists of a sequence of convolutional layers connected in a special way. Each dense block in DenseNet-121 is made up of a number of layers, often with three different sorts of operations: batch normalization, ReLU activation, and 3x3 convolutional layer. The fact that each layer inside a dense block receives the feature maps from all preceding layers as input, however, is what really sets DenseNet apart. Before being input into the following layer, these feature maps are concatenated along the depth dimension. Because of the gradients and information flow that are facilitated by the dense connectivity, learning complicated patterns in the data is made simpler for the network. Dense connections also promote feature reuse and solve the vanishing gradient issue, making the model more parameter-efficient

- *Transition Layer*

In order to limit the number of feature maps and control the spatial dimensions and hence the computational cost, transition layers are inserted between dense blocks. A 1x1 convolutional layer, average pooling, and a decrease in the spatial dimensions make up a typical transition layer.

- *Growth Rate*

Each layer in a dense block contributes a certain number of feature mappings to the following layer, which is determined by the growth rate parameter. It regulates the model's capability and the rate of layer addition growth. Depending on the particular task and dataset, the growth rate is frequently a hyperparameter that can be adjusted.

- *Bottleneck Layers*

Before each 3x3 convolutional layer in a dense block, a bottleneck layer can be added to further cut down on computing expenses. Before performing the more computationally demanding 3x3 convolution, the bottleneck layer reduces the amount of input feature maps using a 1x1 convolution.

- *Global Average Pooling and Softmax*

Global average pooling is used to transform the 4D tensor output into a 2D feature matrix after the last dense block. For classification, this matrix is subsequently fed into a fully linked softmax layer. The feature maps' spatial dimensions are reduced to a constant size thanks to global average pooling, which enables the network to handle inputs of various sizes.

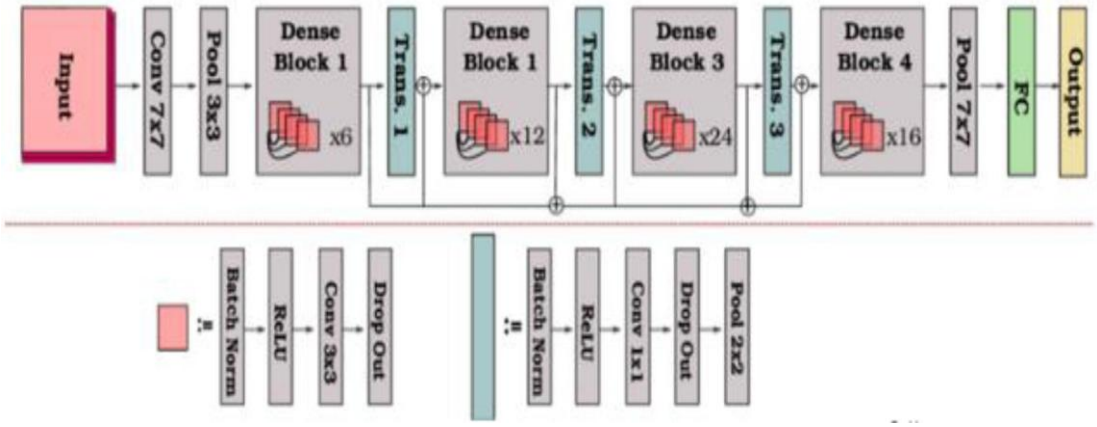

Figure 6: DenseBlock and transition layer [119]

4.4 Ensemble Scheme

Several classification algorithms are merged into one model in the Ensemble ML paradigm. In this study, we used soft voting to merge the results of three classification models. As a result, the proposed scheme produces the following result eq 4.1:

$$f_{comb}(x_n) = \sum_{t=1}^{T} \alpha_t f_t(x_n),\ f_t \in [0,1],$$

Suppose we have t number of base classifiers h_t, which are trained with classifier specific weights α_t. Let $f_t(x_n)$ represents the output of tth classifier for input (xn). Where $f_{comb}(x_n)$ is the weighted linear combination of the T base classifier, α_t is the weight for the classifier h_t.

5. EVALUATION METRICS

On the two chest illness datasets, the proposed method was assessed using four conventional assessment criteria: accuracy (Acc), precision (Pre), recall (Rec), and f1-score (F1). We'll start by defining the terms "True Positive," "False Positive," "True Positive," "False Negative," and the expressions "True Positive," "False Negative," and so on. Think of a binary classification task where the dataset is divided into "positive" and "negative" classes. The definitions of the terms stated above are provided below. True Positive refers to a positive-class sample that a model has accurately classified (TP). False positives are samples that should have been classified as negative but were instead positive (FP).

A True Negative is a sample that the model correctly identifies as being in the negative category (TN). False negatives are samples that should have been categorized as negative but were instead categorized as positive (FN). Result matrices are shown in eq 4.2, 4.3, 4.4, 4.5.

$$\text{Accuracy} = \frac{\text{Total correct predictions}}{\text{Total cases}}$$

$$\text{Recall or Sensitivity} = \frac{\text{Total Correct positive predictions}}{\text{Total Positive cases}}$$

$$\text{Precision} = \frac{\text{Total correct positive predictions}}{\text{Total positive predictions}}$$

$$\text{F1 score} = 2 * \frac{\text{Precision} * \text{Recall}}{\text{Precision} + \text{Recall}}$$

6. RESULTS AND DISCUSSION

In this section, we present an analysis of the "RGDSoft" system as proposed. As detailed in the preceding section, the RGDSoft system consists of three classifiers ResNet18, GoogleLeNet, and DenseNet-121 ensemble with Soft-voting. This system was applied to two publicly available datasets of chest radiographs for the detection of new coronaviruses (COVID-19) and pneumonia. To showcase the effectiveness of the proposed system, a comparison was made against various ensemble models. The performance of the RGDSoft model on the Kermany dataset is illustrated in Fig 4, achieving a remarkable 98.81% accuracy, 98.82% precision, 98.8% recall, and 98.79% F1 score.

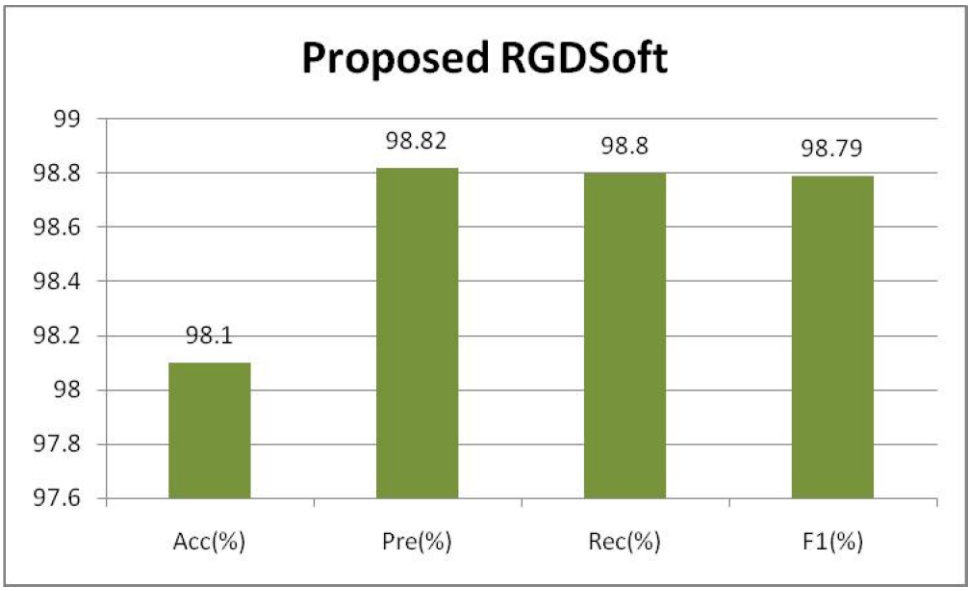

Figure 7: Performance analysis of RGDSoft on the kermany dataset

Accuracy attained by RGDSoft on kermany dataset is compared with some pre- trained models and some standard models presented in the literature. Figure 7 clearly shows proposed RGDSoft model outperformed all the models and achieved an overall accuracy of 98.1%.

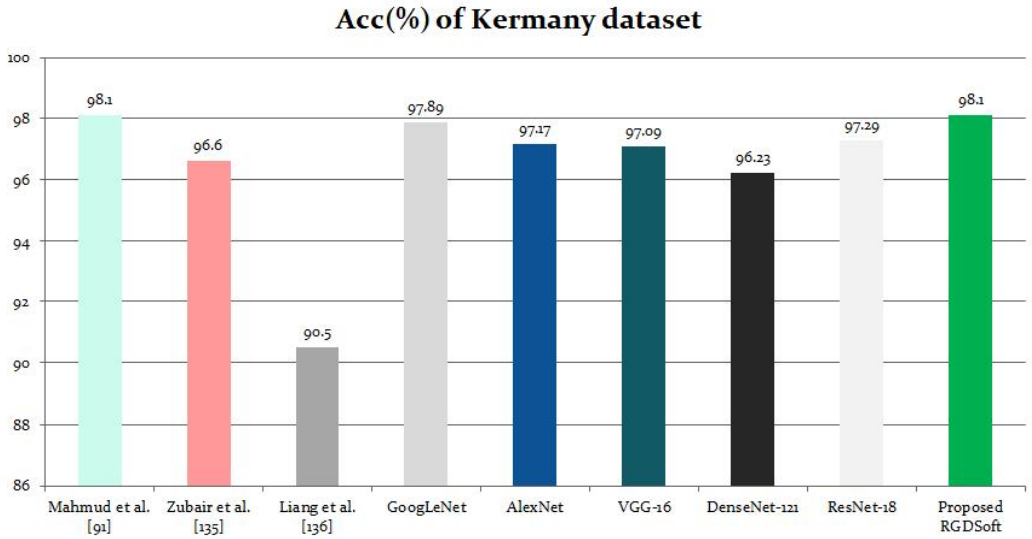

Figure 8: Accuracy comparison on kermany dataset

Precision attained by RGDSoft on kermany dataset is compared with some pre- trained models and some standard models presented in the literature. Figure 9 clearly shows proposed RGDSoft model outperformed all the models and achieved a precision of 98.82%.

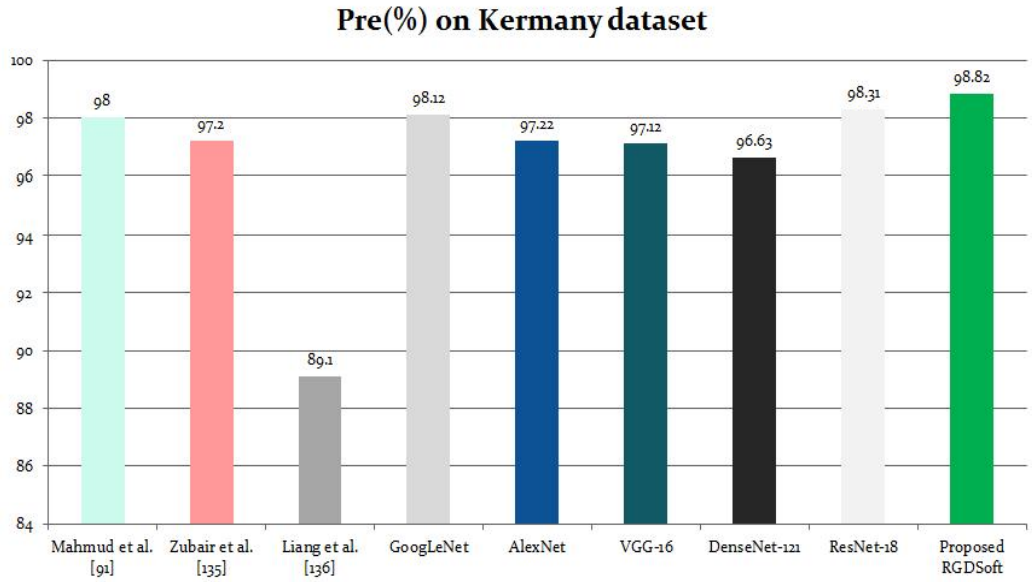

Figure 9: Precision comparison on kermany dataset

Recall attained by RGDSoft on kermany dataset is compared with some pre-trained models and some standard models presented in the literature. Figure 10 clearly shows proposed RGDSoft model outperformed all the models and achieved a recall of 98.79%.

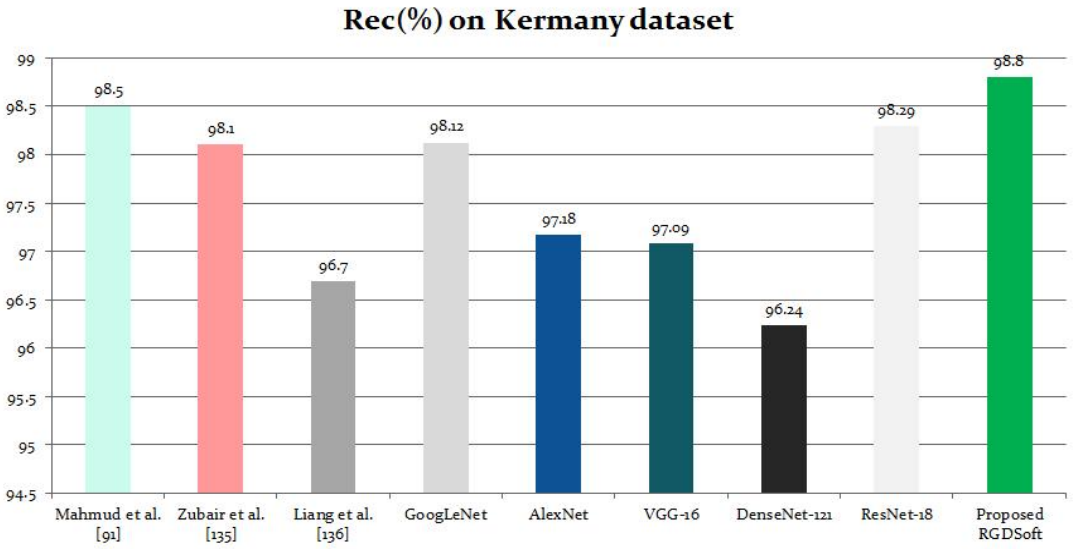

Figure 10: Recall comparison on kermany dataset

F1 score attained by RGDSoft on kermany dataset is compared with some pre- trained models and some standard models presented in the literature. Fig 11 clearly shows proposed RGDSoft model outperformed all the models and achieved an F1 score of 98.82%.

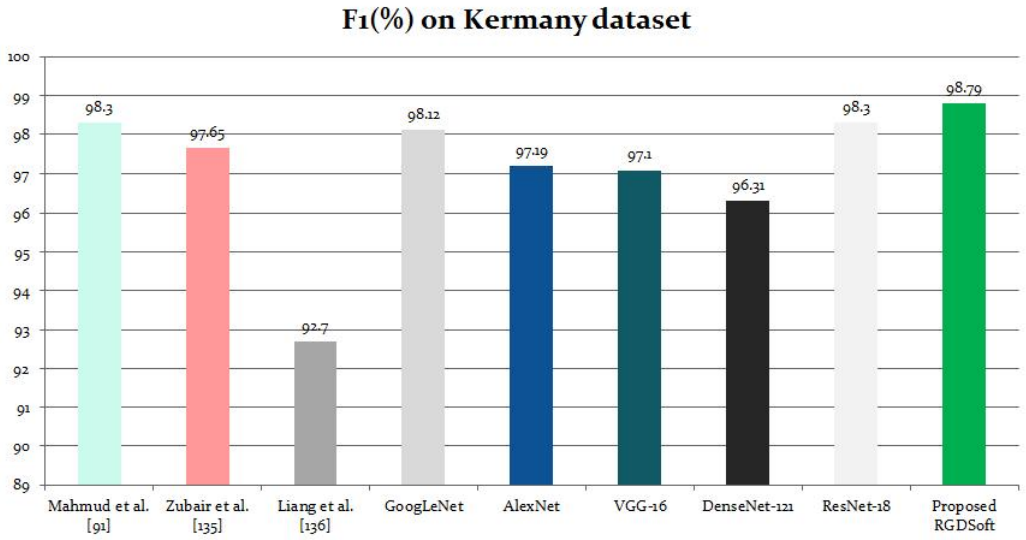

Figure 11: F1 score comparison on kermany dataset

Figure 12 summarizes the whole result analysis of the RGDSoft model with state- of-the-art models and clearly shows a much better result, which makes it the top model among all others; our suggested model has surpassed all other models.

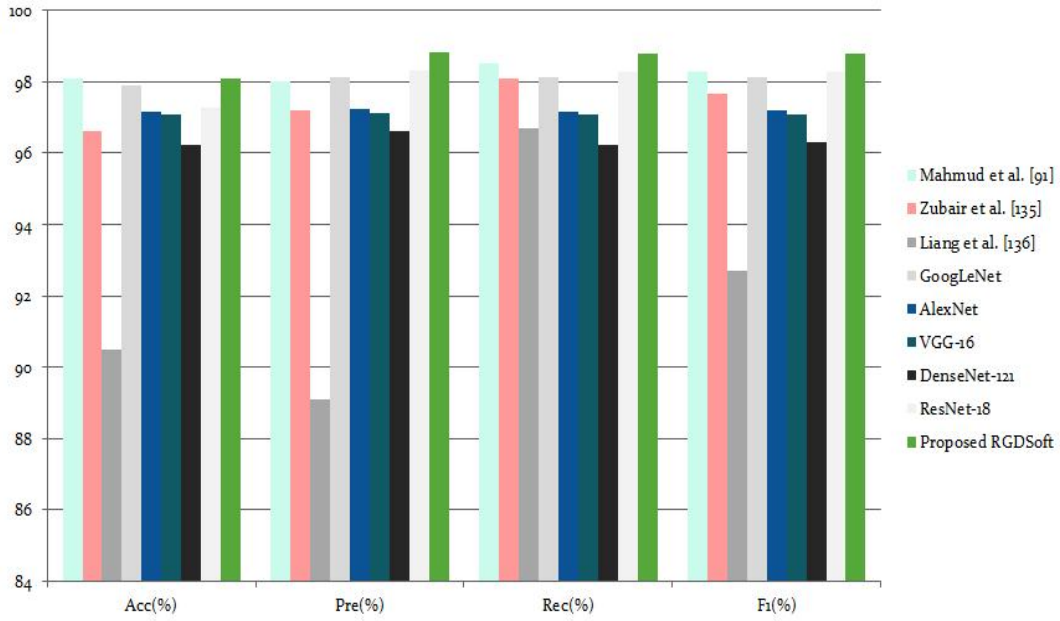

Figure 12:Performance analysis of the proposed RDGSoftmodel with other models on Kermany dataset [135]

Figure 13 shows the performance results of the RGDSoft model on the Covid-19 dataset. The proposed model has given 94% accuracy, 96% precision, and 96% recall.

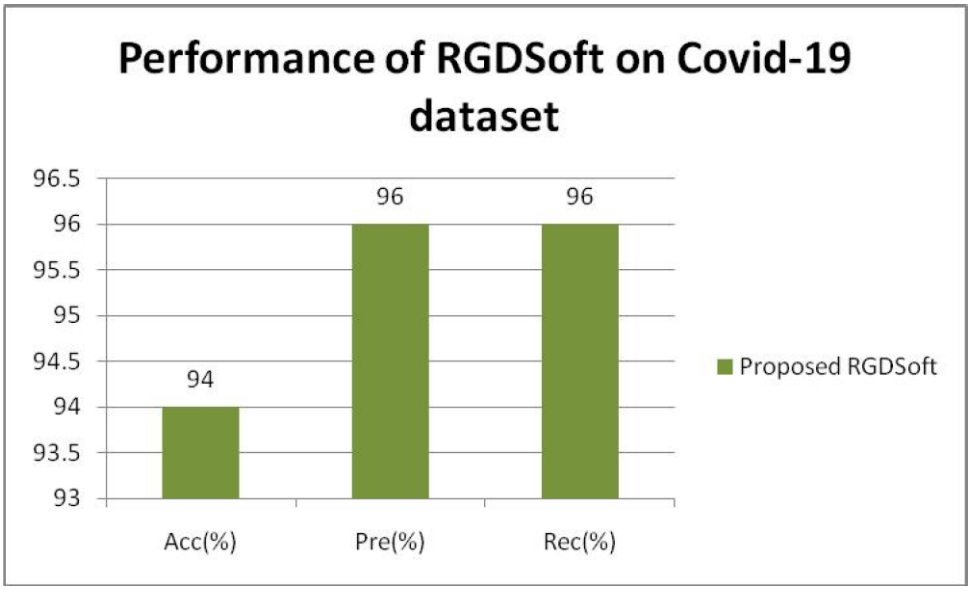

Figure 13: Performance analysis of RGDSoft on Covid-19 dataset

Accuracy attained by RGDSoft on covid-19 dataset is compared with some pre- trained models and some standard models presented in the literature. Figure 14 clearly shows proposed RGDSoft model outperformed all the models and achieved an overall accuracy of 94%.

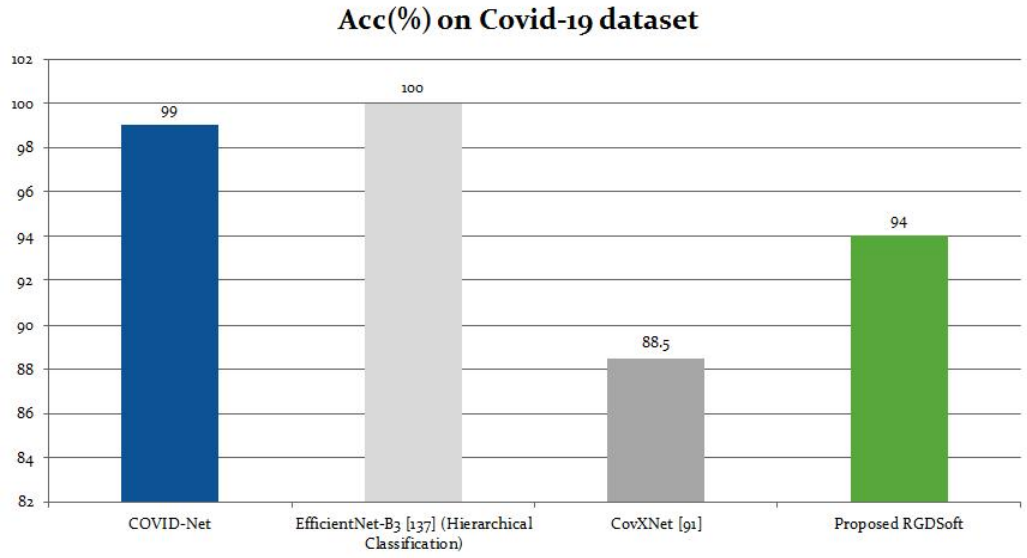

Figure 14: Accuracy comparison of the COVID-19 dataset

Precision attained by RGDSoft on covid-19 dataset is compared with some pre- trained models and some standard models presented in the literature. Figure 15 clearly shows proposed RGDSoft model outperformed all the models and achieved a precision of 96%.

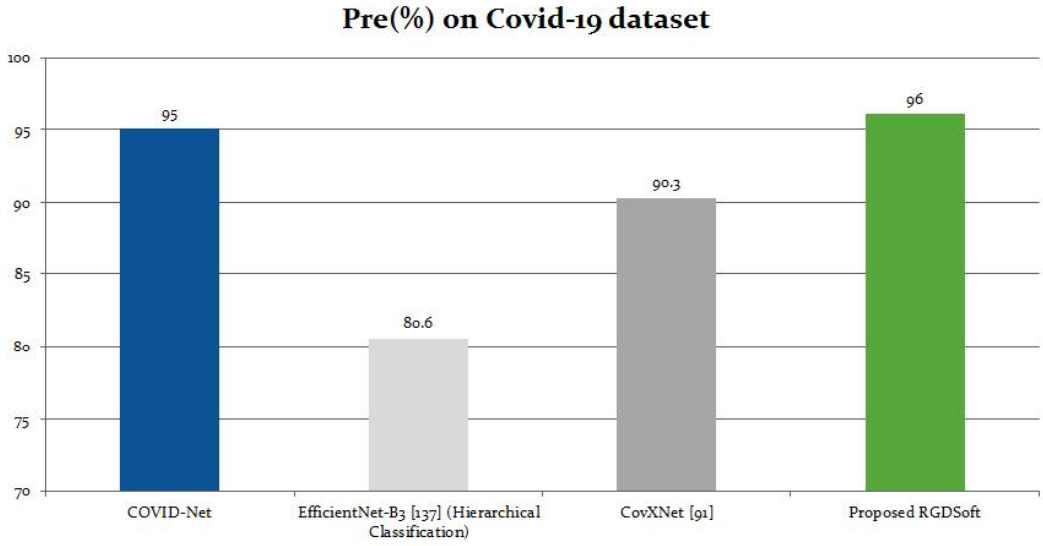

Figure 15: Precision comparison of the COVID-19 dataset

Recall attained by RGDSoft on covid-19 dataset is compared with some pre-trained models and some standard models presented in the literature. Figure 16 clearly shows proposed RGDSoft model outperformed all the models and achieved an overall accuracy of 96%.

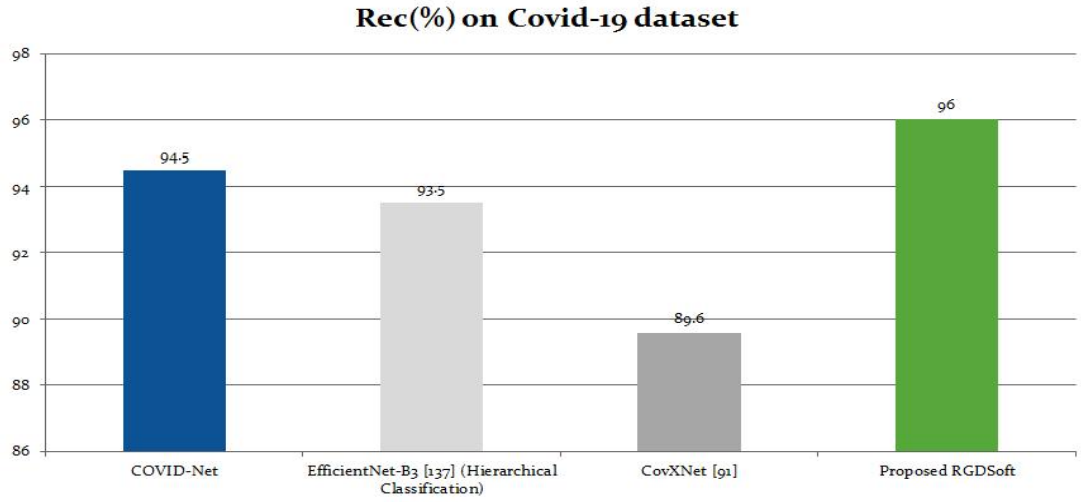

Figure 16: Recall comparison on the Covid-19 dataset

On the Covid-19 datasets, the results of the proposed RGDSoft mode analysis with other current models are pictorial representations in Figure 17. Here, it is clear that with 94% accuracy, 96% precision, and 96% recall, our suggested RGDSoft model performs better than several cutting-edge models. If applied to a different dataset, the comparable models that display nearly 100% accuracy are over-fitted and will produce very poor results. This makes it abundantly evident that our suggested model is general in nature and that it can be used on many datasets to outperform its rivals in terms of actual results.

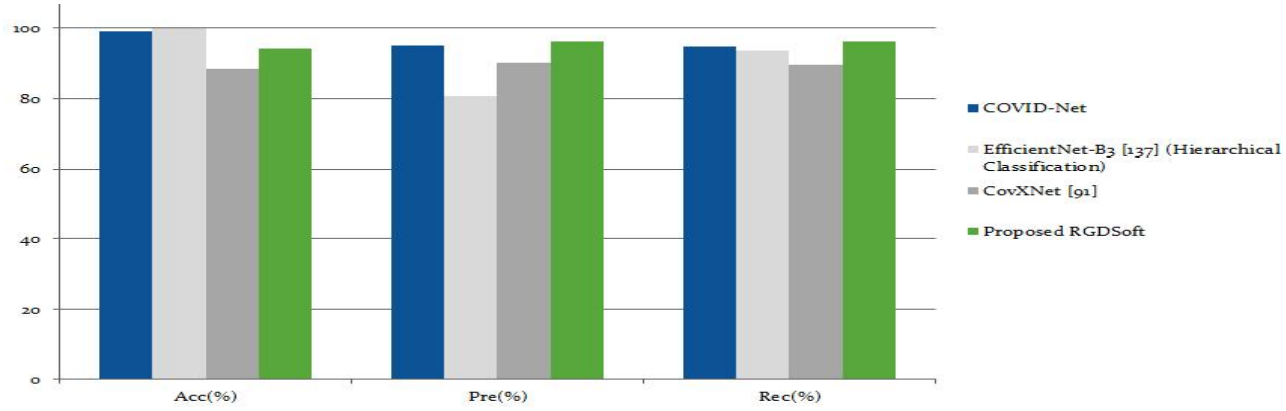

Figure 17: The proposed method was contrasted with the current ones. Regarding the COVID-19 dataset

7. SUMMARY

In order to diagnose lung diseases like COVID-19 and pneumonia from chest X-ray pictures, this study presented an ensemble approach called RGDSoft. The suggested ensemble model works better and captures COVID-19 infection more accurately when compared to other well-known techniques. The decision scores of the three CNN models, GoogLeNet, ResNet-18, and DenseNet-121, were combined to construct a soft voting ensemble. Our methodology was applied to the Kermany dataset as well as the Covid-19 dataset. On the Covid-19 dataset, we achieved 94% accuracy, 96% precision, and 96% recall while outperforming the majority of cutting-edge models. On the Kermany dataset, with 98.1% accuracy, 98.82% precision, 98.80% recall, and 98.79% f1 score. Similar to this, the recommended ensemble model's generality makes it applicable to a wide range of computer vision problems.

REFERENCES

[1] Schroeder JD, Bigolin Lanfredi R, Li T, Chan J, Vachet C, Paine III R, Srikumar V, Tasdizen T. Prediction of obstructive lung disease from chest radiographs via deep learning trained on pulmonary function data. International Journal of Chronic Obstructive Pulmonary Disease. 2020 Jan 5:3455-66.

[2] Xiong Y, Ba X, Hou A, Zhang K, Chen L, Li T. Automatic detection of mycobacterium tuberculosis using artificial intelligence. Journal of thoracic disease. 2018 Mar;10(3):1936.

[3] Gonzalez G, Ash SY, Vegas-Sánchez-Ferrero G, Onieva Onieva J, Rahaghi FN, Ross JC, Díaz A, San José Estépar R, Washko GR. Disease staging and prognosis in smokers using deep learning in chest computed tomography. American journal of respiratory and critical care medicine. 2018 Jan 15;197(2):193-203.

[4] Liu W, Liu M, Guo X, Zhang P, Zhang L, Zhang R, Kang H, Zhai Z, Tao X, Wan J, Xie S. Evaluation of acute pulmonary embolism and clot burden on CTPA with deep learning. European radiology. 2020 Jun;30:3567-75.

[5] walsh SL, Calandriello L, Silva M, Sverzellati N. Deep learning for classifying fibrotic lung disease on high-resolution computed tomography: a case-cohort study. The Lancet Respiratory Medicine. 2018

[6] Demir F, Sengur A, Bajaj V. Convolutional neural networks based efficient approach for classification of lung diseases. Health information science and systems. 2019 Dec 23;8(1):4.

[7] Gite S, Mishra A, Kotecha K. Enhanced lung image segmentation using deep learning. Neural Computing and Applications. 2023 Nov;35(31):22839-53.

[8] Zak A classification of lung diseases using deep learning models. In International Conference on Computational Science 2020 Jun 3 (pp. 621-634). Cham: Springer International Publishing. [80] Sriporn K, Tsai CF, Tsai CE, Wang P. Analyzing lung disease using highly effective deep learning techniques. InHealthcare 2020 Apr 23 (Vol. 8, No. 2, p. 107). MDPI.

[9] Yimer F, Tessema AW, Simegn GL. Multiple Lung Diseases Classification from Chest X-ray Images using Deep Learning approach. Int. J. 2021 Sep;10:2936-46

[10] Madhuri S, Mahesh TR, Vivek V, Shashikala HK, Saravanan C. Analysis and Design for the Early Stage Detection of Lung Diseases Using Machine Learning Algorithms. Data Engineering and Data Science: Concepts and Applications. 2023 Sep 15:351-71.